coatings

MDPI

Article

Experimental Study on Neutral Salt Spray Accelerated Corrosion of Metal Protective Coatings for Power-Transmission and Transformation Equipment

Junwei Chen [1,†], Jie Liu [2,†], Haobin Wang [2], Bo Li [1], Quan Hu [1], Tianjing Shao [3], Ruijing Yang [3], Bin Wang [3], Qiang Wan [2], Zhenggang Li [2,*], Yan Lei [2], Guodong Zhang [2] and Bing Yang [2,4,*]

1 Electric Power Research Institute of Guizhou Power Grid Co., Ltd., Guiyang 550000, China
2 School of Power and Mechanical Engineering, Wuhan University, Wuhan 430072, China
3 Xingyi Power Supply Bureau of Guizhou Power Grid Co., Ltd., Xingyi 562400, China
4 International Joint Research Center for Surface and Interface Materials Science and Engineering, Wuhan University, Wuhan 430072, China
* Correspondence: zgli@whu.edu.cn (Z.L.); toyangbing@whu.edu.cn (B.Y.); Tel.: +86-136-0717-8142 (B.Y.)
† These authors contributed equally to this work.

Abstract: At present, the common protection technology of power-transmission and transformation equipment is mainly coating protection and hot-dip zinc protection. However, due to the low adhesion of epoxy zinc-rich coating, and the poor compatibility with top paint, environmental pollution, complex processing, high energy consumption and other defects of the hot-dip zinc process, its development is limited. In view of the above deficiencies, new anti-corrosion coating materials and processes were investigated in this study. Zinc coatings and *Al-Zn* coatings were prepared on the C45 steel matrix by hot-spraying and cold-spraying processes. The macro appearance, micromorphology and phase composition analysis of the coatings were evaluated. The adhesion of the coating to the substrate after the salt-spray test was tested. The results showed that the hot dip zinc coating and hot spray zinc coating had obvious cracking after the salt-spray test. The surface structure of cold-sprayed *Al-Zn* coating was relatively dense after the salt-spray test. The critical load of the cold-sprayed *Al-Zn* coating after the salt-spray test was higher than that of the other two coatings. The corrosion resistance to salt spray of cold-sprayed *Al-Zn* coating was demonstrated to be better than the hot-dip zinc coating, and thus has great application prospects.

Keywords: protective coating; salt-spray corrosion; composition analysis; adhesion; cold spray

check for updates

Citation: Chen, J.; Liu, J.; Wang, H.; Li, B.; Hu, Q.; Shao, T.; Yang, R.; Wang, B.; Wan, Q.; Li, Z.; et al. Experimental Study on Neutral Salt Spray Accelerated Corrosion of Metal Protective Coatings for Power-Transmission and Transformation Equipment. *Coatings* **2023**, *13*, 480. https://doi.org/10.3390/coatings13030480

Academic Editor: Cecilia Bartuli

Received: 10 January 2023
Revised: 13 February 2023
Accepted: 18 February 2023
Published: 21 February 2023

Copyright: © 2023 by the authors. Licensee MDPI, Basel, Switzerland. This article is an open access article distributed under the terms and conditions of the Creative Commons Attribution (CC BY) license (https://creativecommons.org/licenses/by/4.0/).

1. Introduction

Metal materials are the most important structural materials in power-transmission and transformation systems. The base, tower, cabinet and unit of power-transmission and transformation equipment are mainly made of steel components. After a long time of operation in a highly corrosive environment, several serious corrosion problems often occur, which seriously affects the safe operation of the power grid and leads to a number of power-supply accidents [1]. Among them, atmospheric corrosion accounts for more than half of the total corrosion of the tower [2]. Therefore, it is particularly important to study the corrosion of power-transmission and transformation equipment to strengthen its protection and ensure the safe and reliable operation of the transmission system [3]. The main corrosion-failure forms of power-transmission and transformation equipment are pitting corrosion, local corrosion, uniform corrosion, stress corrosion, fatigue corrosion, wear corrosion and chemical corrosion [4]. Xu et al. [5] pointed out that steel frame, aluminum wire, equipment shell, contacts and other metal materials were easily corroded under the environment of hot and humid ocean and industrial air pollution, which affected the safety of the transmission network. Li et al. [6] showed that long-term high temperature,

humidity and salinity could significantly promote the corrosion of metal materials in equipment. Valverde et al. [7] found that the transmission towers in power equipment were more prone to atmospheric corrosion if they were in an atmospheric environment for a long time. Wang et al. [8] found that the corrosion of Cl^- in atmosphere brought more serious corrosion damage to metals and even affected their service life.

Corrosion protection measures for power transmission and transformation equipment include coating protection technology, hot dip galvanizing protection technology, thermal spraying protection technology, electrochemical protection, corrosion-resistant materials and so on [9,10]. On-site temperature, relative humidity and other climatic factors as well as pollutant deposition will affect the corrosion behavior of the coating of power transmission and transformation equipment [5]. Field exposure test is a common method to study atmospheric corrosion, but this method has a long experimental period, which is not conducive to the rapid evaluation of coating properties. The current mainstream method of accelerating the corrosion process is indoor accelerated corrosion test [11,12], in which the salt-spray accelerated corrosion test has a better effect [13,14]. The salt-spray corrosion test of metal materials is conducted to obtain the corrosion resistance by accelerating the simulation of the corrosion of Cl^- in the atmosphere. Jermain et al. [15] and Qing et al. [16] carried out salt-spray accelerated corrosion test on zinc and found that Cl^- intensified the corrosion on zinc surface. Some researchers have used salt-spray accelerated corrosion test to simulate the corrosion of zinc in atmospheric environment, and obtained good experimental results. The results showed that the deposition and dissolution of Cl^- on the surface of zinc led to the enhancement of the conductivity of the medium and accelerated the corrosion rate of zinc [17,18]. Cl^- in an atmospheric environment seriously affects the corrosion resistance of metal materials. The salt-spray accelerated corrosion test can quickly obtain the relevant data of metal corrosion, but there is a lack of research on the corrosion mechanism of new metal protective coatings, such as cold-spray zinc. Wang Qiang et al. prepared pure *Al* and *Al-Zn* composite coatings with excellent properties on the surface of Q345R using cold-spraying technology. The results showed that the cold-sprayed pure *Al* and *Al-Zn* composite coatings were well combined with the Q345R steel substrate, and there were no obvious holes and cracks at the interface. With the increase in *Zn* content, the compacting effect on the coating is strengthened, and the compactness of the coating is improved, so that the mechanical properties of the coating are improved. Jia Li et al. prepared *Al*-zinc coating by cold spraying process. The results showed that the self-corrosion potential of coating was significantly higher than that of magnesium alloy substrate, and the self-corrosion current density was significantly lower than that of magnesium alloy, which could provide good protection for magnesium alloy.

Through a neutral salt-spray accelerated corrosion test, this work systematically studies the corrosion behavior and mechanism of cold spray aluminum zinc, hot-spray zinc and hot-dip zinc protective coatings used in power transmission and transformation equipment, compares the corrosion resistance of different protective coatings, and provides a theoretical basis for the use and life evaluation of corrosion-resistant coatings for power-transmission and transformation equipment.

2. Experimental

2.1. Materials

C45 steel was selected as the substrate, and a 30 mm × 30 mm sample was processed by wire-cutting machine. Before preparing the coating, the sample should be polished first, cleaned with ultrasonic wave, and finally cleaned and dried with anhydrous ethanol to ensure a smooth surface.

2.2. Coating Preparation

Before the preparation of the hot-dip zinc coating, the surface of the substrate needs to be cleaned, and the oxide, rust and pollutants on the surface of the substrate can be removed by sandblasting. The parameters of sandblasting are as follows: quartz sand is

used as abrasive, the air pressure is 0.5 MPa, and the distance is 150 mm. When hot dip zinc is deposited, the zinc content of the bath is above 99.5%, the temperature should be controlled at 450–500 °C, and the duration is 2–4 min.

Before the preparation of the hot-spray zinc coating, the substrate should be sandblasted. The parameters of sandblasting were as follows: quartz sand was used as an abrasive, the air pressure was 0.5 MPa, the angle was 70°, and the distance was 150 mm. The compressed air was kept clean and dry, and the quartz sand was clean and angular. Substrate surface pretreatment should not only remove the rust and oxide layer, but also increase the roughness of the substrate surface, so that the coating can better adhere to the substrate. In this paper, XDP-2 arc-spraying equipment (Beijing, China) was used to arc-spray zinc on the surface of C45 steel samples. The main process parameters of arc spraying are as follows: the arc voltage is 28 V, the arc current is 300 A, the wire feeding voltage is 15 V, the spraying gas is air, the carrier gas pressure is 5–7 MPa and the spraying distance is 150 mm.

The cold-spray aluminum zinc coating was made on the cold-air dynamic spraying equipment. Before the preparation of the coating, the substrate should be sandblasted to remove the rust and oxide layer. The process parameters of sandblasting are as follows: quartz sand is used as an abrasive, the air pressure is 0.5 MPa, and the distance is 150 mm. Aluminum powder and zinc powder should be mixed and shaken at a ratio of 17:3. Before spraying the powder, it should be dried at 120 °C for 30 min. The carrier gas of spraying is high-pressure nitrogen. The parameters of the cold-spray aluminum zinc coating are as follows: the loading temperature is 230 °C, the carrier gas pressure is 1.8 MPa, the powder feeding rate is 1.6 g/s and the spraying distance is 20 mm.

2.3. Neutral Salt-Spray Test

The neutral salt-spray test was used to accelerate the indoor aging of three kinds of coatings, namely cold-spray aluminum zinc, hot-spray zinc and hot-dip zinc coatings. Before the formal salt-spray test, the salt-spray pre-test was carried out on the hot-dip zinc, hot-spray zinc and cold-spray aluminum zinc coating so as to determine the specific test cycle and the representative time period within the formal salt-spray test. After the pre-test of the salt spray, the hot-dip zinc, hot-spray zinc and cold-spray aluminum zinc coatings were numbered respectively. The surfaces of the samples were cleaned with acetone to remove oil stains, and then cleaned again with anhydrous ethanol. The salt-spray test was carried out on a DK-40A salt-spray test machine (Guangzhou, China). The operation is here referred to GB 6458-1986 "Neutral Salt-Spray Test of Metal Overburden (NSS Test)". The temperature of the spray test chamber was 35 ± 2 °C, the air pressure was maintained at 1.00 ± 0.01 Kgf/cm^2 and the spray time was 264 h.

2.4. Material Characterizations

The surface and cross-section morphology of the coating was observed by metallographic microscope and high-resolution camera. A scanning electron microscope (SEM, MIRA 3, TESCAN Brno, Ltd., Oxford, UK) was used to observe and analyze the macroscopic appearance and morphology of the coating before and after corrosion, and the test voltage was 10 KV. The composition of the coating and the main elements of corrosion products were analyzed by energy dispersive spectroscopy (EDS, Aztec Energy-X-Max 20, Oxford, UK). The phase composition of the coating was studied using an X-ray diffraction (XRD, XPert Pro, Wuhan, China) with Cu Kα radiation at a scan step of 0.02 and a scan range from 20 to 70 degrees. The adhesion of substrate and coating was tested by friction and wear testing machine and scratch tester. The friction coefficients were evaluated on the ball-on-disk tester (Rtec MFT-5000) under the room temperature and atmospheric pressure. Si_3N_4 balls with a diameter of 6 mm were chosen. The reciprocating sliding test was carried out with a load of 150 N for 15 min. The frequency was 5 Hz and the sliding distance was 5 mm. Each tested sample was weighted before and after the friction test to obtain the wear rate. The corrosion rate and behavior of the coatings during the salt-spray test are

indirectly explored. The corrosion resistance of the coatings was observed by measuring the weight loss of three metal coating samples after the salt-spray test. Before the test, the three metal coating samples were weighed. The corrosion products of the coating samples were removed, cleaned, dried and weighed after the salt-spray test, and the weight loss of the three metal coatings in each period of the salt-spray test was compared. Electrochemical testing technology was used to study the corrosion behavior of the three metal coatings in 3.5% *NaCl* solution, and to explore their corrosion resistance mechanism and properties. The polarization curve and AC impedance spectrum tests were carried out on CHI604E electrochemical station (Beijing, China), which is a typical three-electrode system. The coating sample was the working electrode, the platinum plate was the auxiliary electrode, the silver chloride electrode was the reference electrode and the electrochemical solution was a *NaCl* solution with a mass fraction of 3.5%. During the test, the working electrode was immersed in the electrochemical solution for 30 min until the potential was stable. The working electrode was prepared by cutting a small piece of 5 mm × 6 mm from the three coatings, connecting the back of the coating sample with the copper wire, and then applying cold mosaic. After the completion of the cold mosaic, the sample was removed with acetone, and then cleaned and dried with anhydrous ethanol to ensure the smooth surface of the sample. The polarization curve scanning rate is 10 mV/s and the voltage range is −2.2 V~−0.4 V.

3. Results and Discussion

3.1. Macroscopic Corrosion Morphology

The macroscopic corrosion morphology of the three metal coatings—hot-dip zinc, hot-spray zinc and cold-spray aluminum zinc coatings—after the salt-spray test is shown in Figure 1. The hot-dip zinc and hot-spray zinc coatings had metallic luster before the salt-spray test, and the cold-spray aluminum zinc coating was dark. The surface of the hot-dip zinc coating was rough, with bumps and pits, which were caused by the hot-dip zinc process. The surface of the hot-spray zinc coating was smooth, and the surface of the cold-spray aluminum zinc coating was granular and had obvious lines, because the quality of the *Al* particles sprayed by the cold-spraying machine was different from that of the *Zn* particles. The lighter *Al* particles were the first to attach to the substrate, and then the *Zn* particles covered and impacted the attached *Al* particles [19]. The obvious lines on the surface of the cold-spray aluminum zinc coating occurred because in the preparation process of the cold-sprayed samples, after one spray was completed, the workbench rose a certain distance to continue the next spray according to the set parameters [20].

After the 72 h salt-spray test, the corrosion products of the three metal coatings increased and became dense, which isolated the corrosive medium from the coating and played a good physical shielding role. After 168 h of the salt-spray test, the corrosion products on the surface of the hot-dip zinc and hot-spray zinc coatings were continuously formed and dissolved, and the dissolution rate of the coating corrosion products was faster than the formation rate, which greatly reduced the corrosion products. The amount of spalling and dissolution of corrosion products of the cold-spray *Al-Zn* coating was less than that of the hot-dip *Zn* and hot-spray *Zn* coating, indicating that the physical shielding performance of cold-spray *Al-Zn* coating was the best in the salt-spray test. After 216 h, the surface of the three coatings did not show red rust, indicating that the three coatings still had good protective properties.

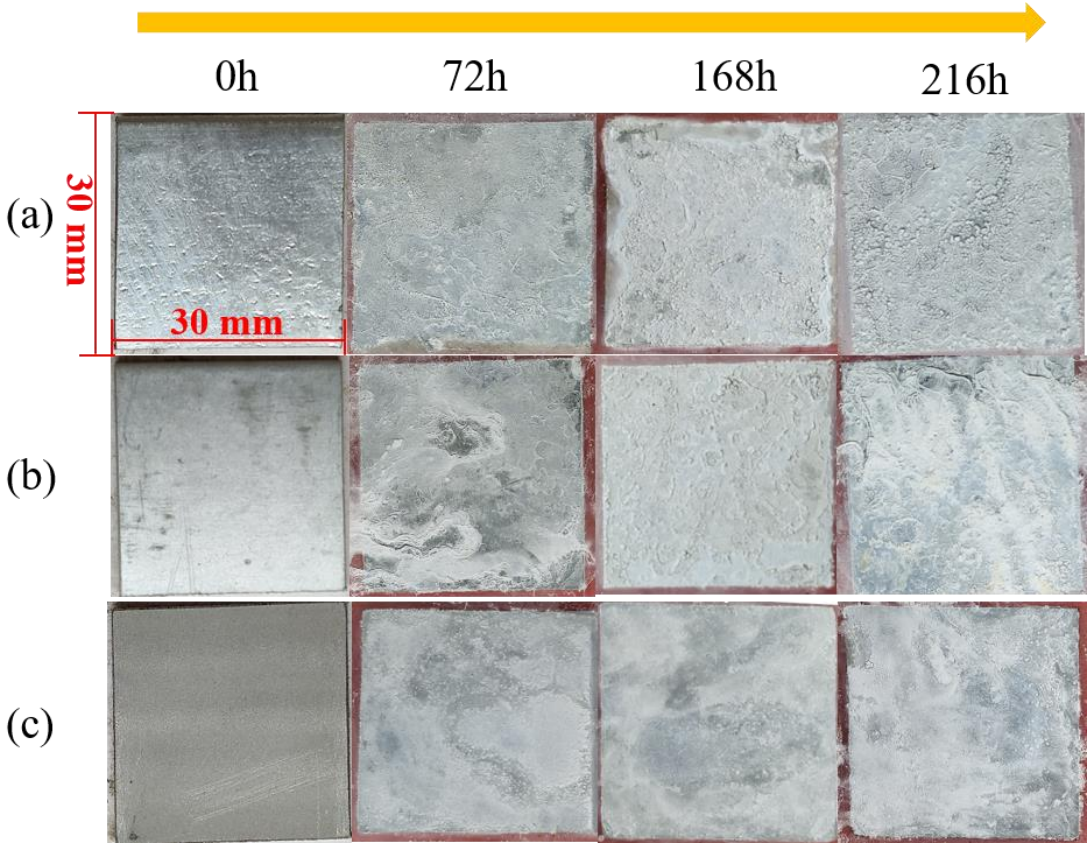


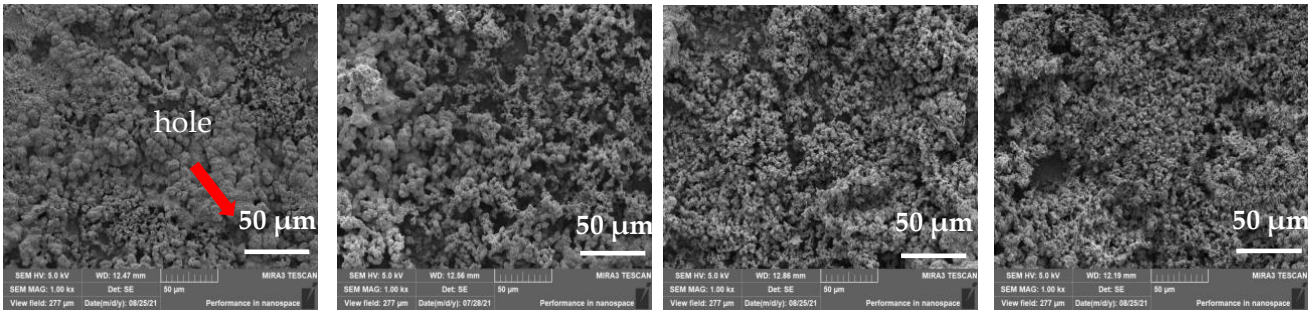
Figure 1. Macroscopic corrosion morphology of three metal coatings after salt-spray test: (**a**) hot-dip zinc coating, (**b**) hot-spray zinc coating and (**c**) cold-spray aluminum zinc coating.

3.2. Microscopic Corrosion Morphology

The SEM images of the surface morphology of the three metal coatings after the salt-spray test are shown in Figure 2. The surface SEM morphology and section of the three metal coatings before salt spray are shown in Figure 3. After salt-spray testing 48 h, serious dissolution occurred on the hot-dip zinc coating. There were many corrosion holes on the coating surface, and a layer of islands and granular corrosion products were formed on the surface. The structure was loose, and the distribution is uneven. The cracks in the grain boundaries of the coating led to obvious cracking and spalling of the corrosion products. With the progress of the salt-spray test, the corrosion dissolution of the hot-dip zinc coating became more and more serious, until the corrosion products were dissolved and spalled at 216 h, leading to a reduction in corrosion products.

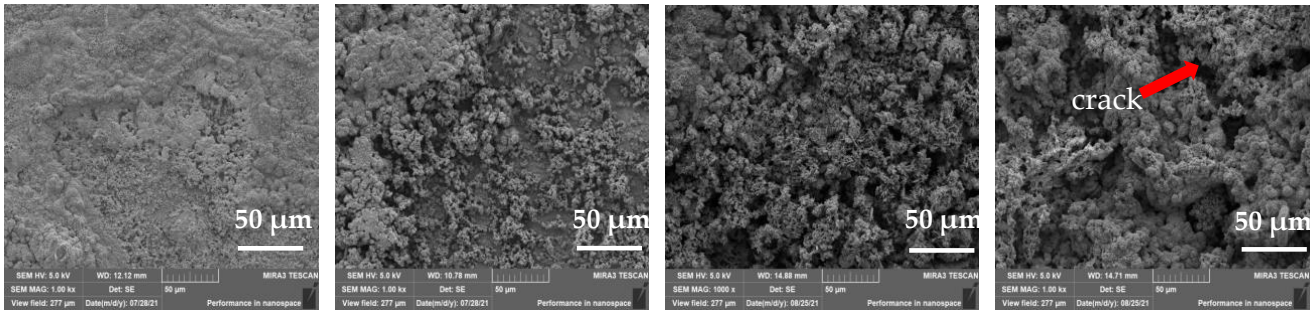
After salt-spray testing 24 h, the surface of the hot-spray zinc coating was almost covered by corrosion products, but the distribution was uneven. After salt-spray testing 72 h, the corrosion products were seriously dissolved and spalled, resulting in a reduction in corrosion products. As the salt-spray test continued, the dissolving phenomenon of the coating became more serious. After 216 h of the salt-spray test, the corrosion products on the coating surface were mostly isolated and granular, and there were obvious cracks. The surface of the cold-spray aluminum-zinc coating was mostly covered by corrosion products with uniform distribution after salt-spray testing for 24 h. Due to the dissolution of corrosion products, there were some small corrosion pits on the surface of the coating. The dissolution and spalling rate of the corrosion products were higher than the formation rate, and the corrosion products on the coating surface were reduced after 72 h of salt-spray testing. With the development of the salt-spray test, the dissolving phenomenon of the coating became more serious. In the salt-spray test lasting 216 h, due to the difference in grain size between *Al* and *Zn* particles, the particle bonding property became weak, and

obvious cracks appeared on the surface of the cold-spray *Al-Zn* coating. The structure was dense, and the corrosion products was mostly flocculent and a few were spinel. The cracks were covered by the flocculent corrosion products, and the corrosion process was prevented by the dense Al_2O_3 film on the coating surface.



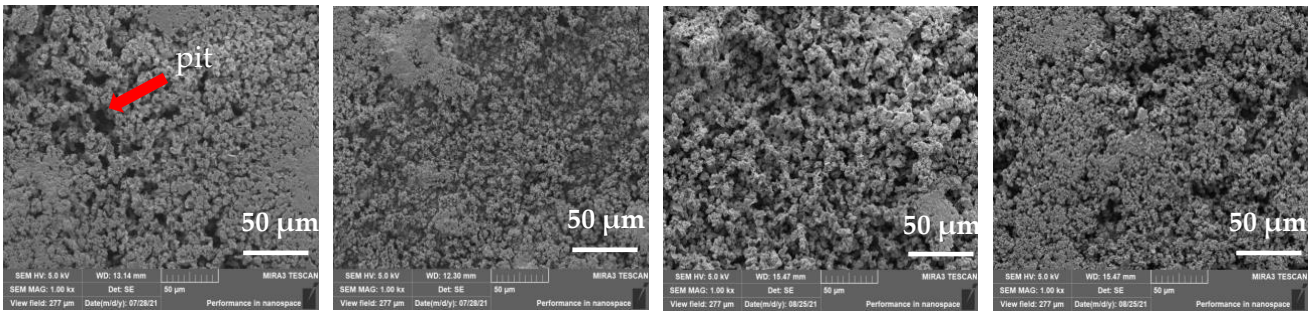
48 h 72 h 120 h 216 h

(**a**)



48 h 72 h 120 h 216 h

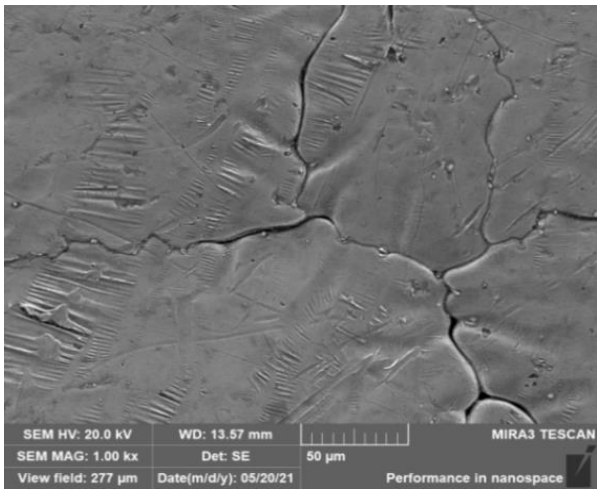
(**b**)



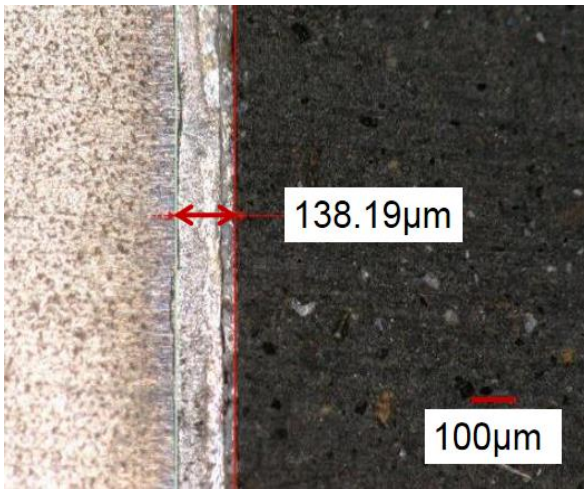
48 h 72 h 120 h 216 h

(**c**)

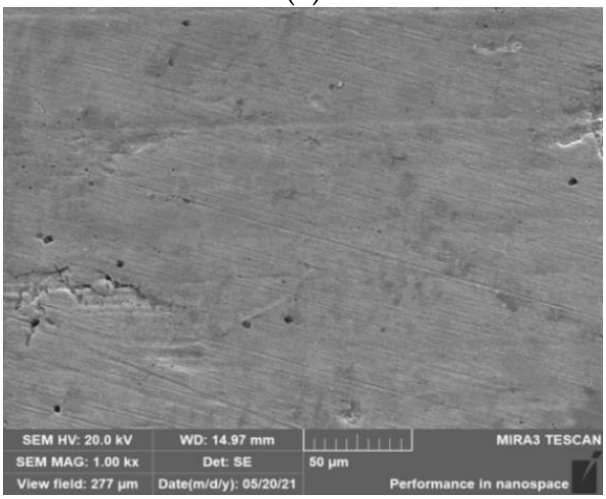
Figure 2. SEM images of surface morphology of three metal coatings after salt-spray test. (**a**) Hot-dip zinc coating, (**b**) hot-spray zinc coating and (**c**) cold-spray aluminum zinc coating.



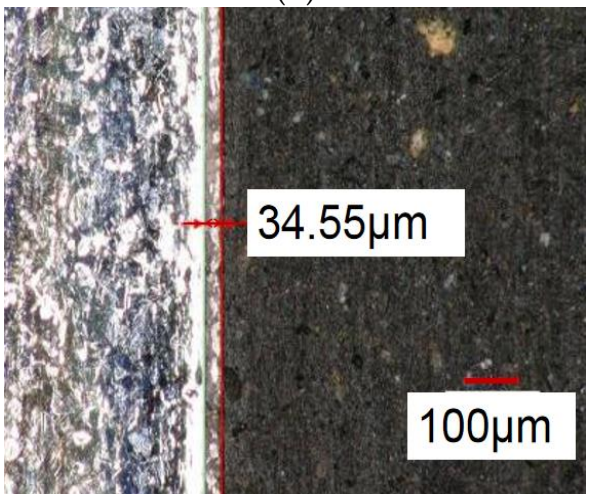
(**a**)



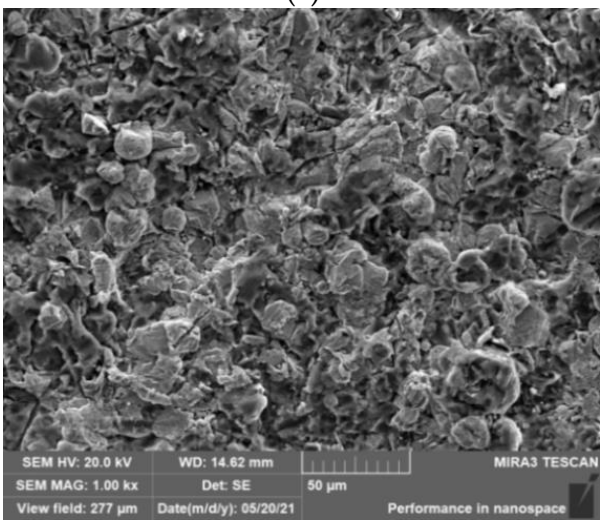
(**b**)



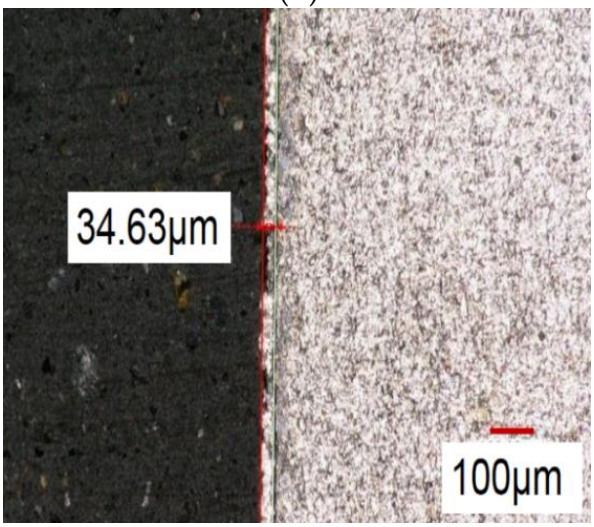
(**c**)



(**d**)



(**e**)



(**f**)

Figure 3. Surface SEM morphology and section of the three metal coatings before salt spray. (**a**) Hot-dip zinc surface SEM, (**b**) hot-dip zinc section SEM, (**c**) hot-spray zinc surface SEM, (**d**) hot-spray zinc section SEM, (**e**) cold-spray aluminum-zinc surface SEM and (**f**) cold-spray aluminum-zinc section SEM.

3.3. Corrosion Products Analysis

The surface EDS analysis of the hot-dip zinc, hot-spray zinc and cold-spray aluminum zinc coatings after the 216 h salt-spray test is shown in Figure 4. The corrosion products of the hot-dip zinc and hot-spray zinc coatings after the 216 h salt-spray test were composed of *Zn*, *O*, *C*, *Na* and *Cl* elements. Among them, *Zn* and *O* were the main elements. It has been shown that the corrosion products of a *Zn* coating after a 216 h neutral salt-spray test are mainly *ZnO* [21]. After 216 h of the neutral salt-spray test, the corrosion products of the cold-spray *Al-Zn* coating were composed of *Al*, *Zn*, *O*, *C*, *Na* and *Cl* elements, among which *Zn*, *Al* and *O* were the main elements. Relevant studies have shown that the corrosion products of the cold-spray *Al-Zn* salt-spray test are mainly $Zn(OH)_2$ and $Zn_5(OH)_8Cl_2{\cdot}H_2O$, and they also contain small amounts of $Al(OH)_3$, Al_2O_3 and *ZnO* [22]. It has been shown that $Zn_5(OH)_8Cl_2{\cdot}H_2O$ is a lamellar crystalline product with a preferred arrangement on the surface of the coating, thus forming a tight product layer to increase the shielding effect of the coating and the path of penetration of the corrosive medium into the substrate, thus increasing the corrosion resistance of the coating [23]. The content of *Al* in the cold-spray *Al-Zn* coating was very high, and the corrosion products of *Al* appeared after the salt-spray test. In the corrosion process, *Al* oxide was formed on the surface, and its compactness and stability led to the improvement of the corrosion resistance of the coating [24,25]. After 216 h of salt-spray test, the presence of *Na* in the three coatings was because the *Na* in the salt spray became attached to the coating.

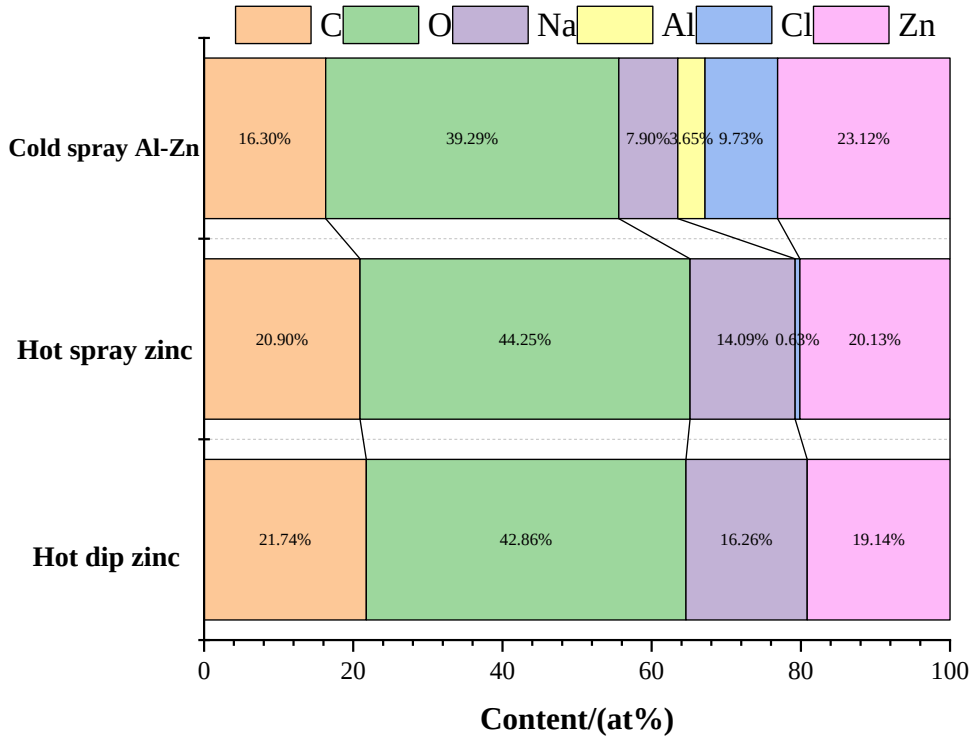


Figure 4. Surface EDS analysis of hot-dip zinc, hot-spray zinc, and cold-spray aluminum zinc coatings after 216 h salt-spray test.

XRD patterns of the three metal coatings after the salt-spray test are shown in Figure 5. As can be seen from Figure 5, the hot-dip zinc and hot-spray zinc coatings after salt-spray test were composed of *Zn*, *ZnO*, $Zn(OH)_2$ and $Zn_5(OH)_8Cl{\cdot}H_2O$ phases. The cold-spray *Al-Zn* coating was composed of *Zn*, *Al*, *ZnO*, Al_2O_3, $Zn(OH)_2$ and $Zn_5(OH)_8Cl{\cdot}H_2O$ phases. The main source of the Al_2O_3 phase was the oxidation of the sample in the air. During the production process, the samples either undergo oxidation reaction in the air, or $Zn(OH)_2$ is dehydrated in a dry environment to form *ZnO* [26]. The Cl^- ions in the salt spray react

with ZnO and $Zn(OH)_2$ to form $ZnCl_2$, and then react with ZnO to form $Zn_5(OH)_8Cl$ [27]. The content of phase components in the XRD pattern was related to the level and number of corresponding peaks. The higher or more closely corresponding the peaks were, the higher the content of the phase components on the surface of the corroded coating. Therefore, the main phases of the hot-dip zinc and hot-spray zinc coatings were Zn and ZnO, while the main phases of the cold-spray Al-Zn coating were Zn, $Zn(OH)_2$ and $Zn_5(OH)_8Cl_2{\cdot}H_2O$.

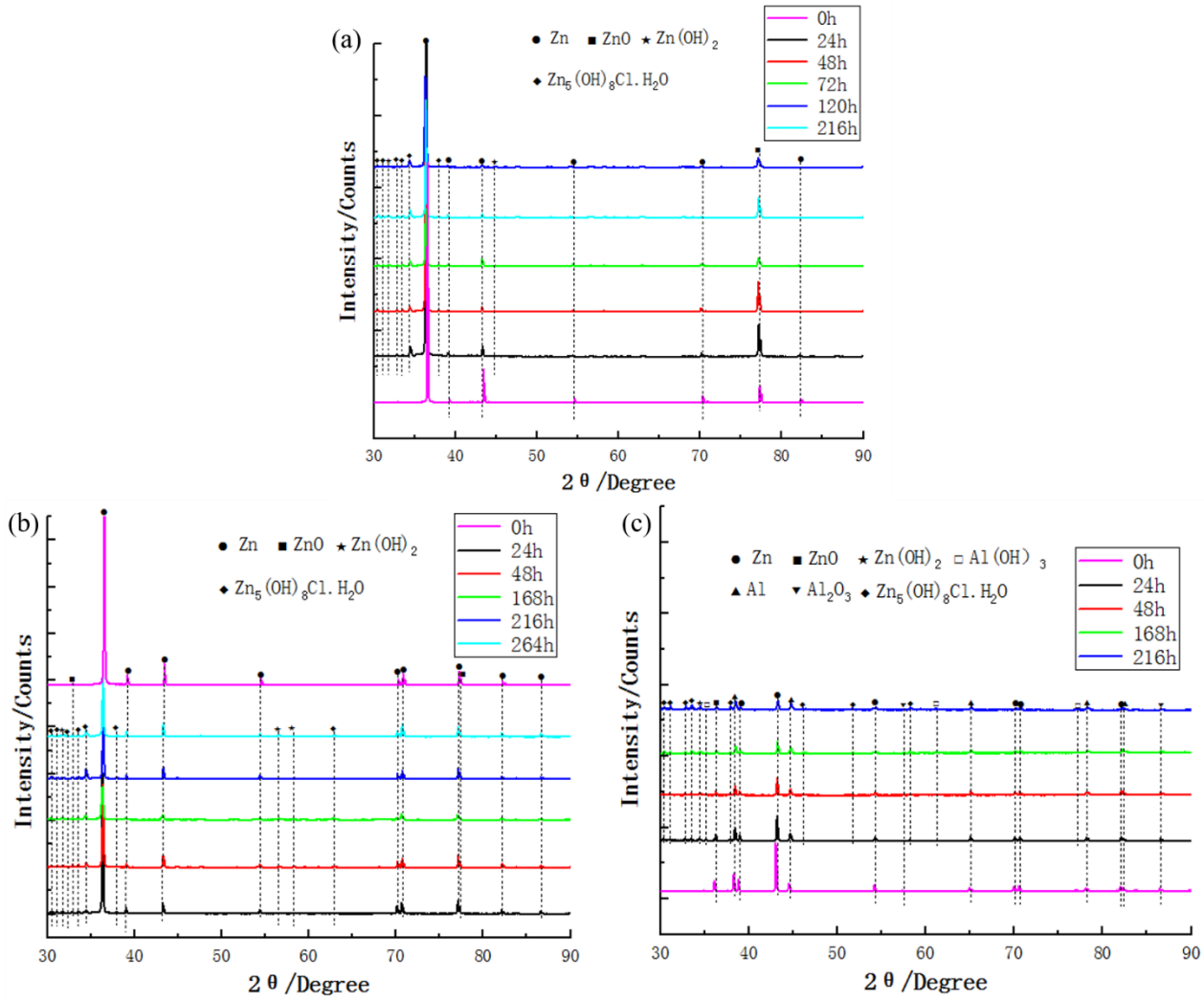


Figure 5. XRD patterns of the three metal coatings after salt-spray test. (**a**) Hot dip zinc, (**b**) hot-spray zinc and (**c**) cold-spray aluminum zinc coatings.

The corrosion resistance mechanisms of coating in a salt-fog environment are shown in Figure 6. The corrosion mechanism and corrosion behavior of the zinc and aluminum-zinc coatings can be analyzed. When the hot-dip zinc and hot-spray zinc coatings are in the salt-spray environment, corrosion protection mainly depended on physical shielding and cathodic protection of zinc coating. The reaction formulas are as follows [28]:

Anodic reaction:

$$Zn \rightarrow Zn^{2+} + 2e^{-} \quad (1)$$

Cathodic reaction:

$$O_2 + 2H_2O + 4e^{-} \rightarrow 4OH^{-} \quad (2)$$

Total reaction:

$$2Zn + 2H_2O + O_2 \rightarrow 2Zn(OH)_2 \quad (3)$$

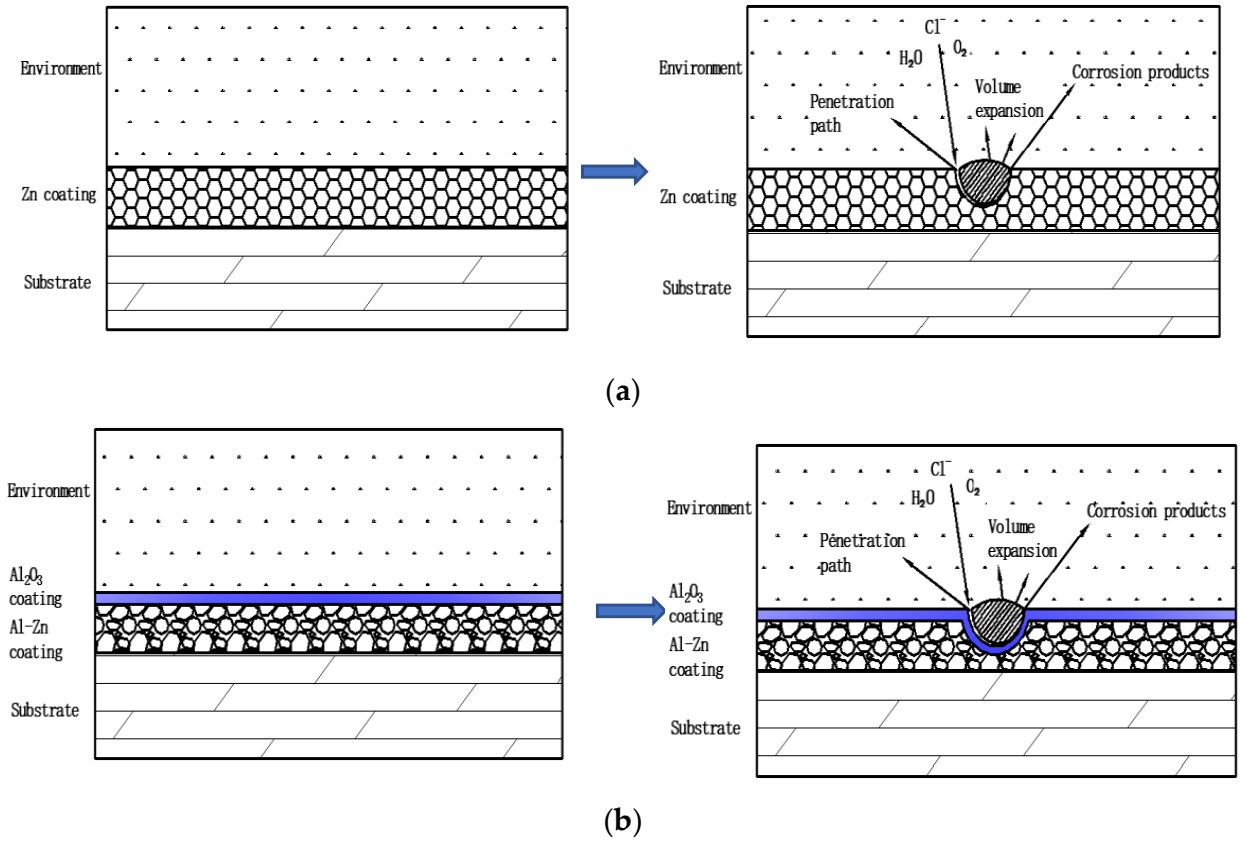


Figure 6. Corrosion resistance mechanism of coating in salt-fog environment. (**a**) Zinc coating and (**b**) aluminum zinc coating.

As the salt-spray test continued, the content of OH^- on the coating surface gradually increased, and $Zn_5(OH)_8Cl_2$ was finally formed. The reaction equation is as follows [29]:

$$Zn(OH)_2 + 4Zn^{2+} + 6OH^- + 2Cl^- \rightarrow Zn_5(OH)_8Cl_2 \quad (4)$$

The corrosion protection of cold-spray *Al-Zn* coating in a salt-spray environment is the same as that of zinc coating, which mainly depends on the physical shielding and cathodic protection of the coating [30]. At the initial stage of the salt-spray test, the protection of the coating is mainly the cathodic protection of zinc, and the Equations (1)–(3) of zinc coating are shown in this case. When the zinc particles on the coating surface are corroded and consumed, the aluminum particles gradually react. The reaction equations are as follows [31]:

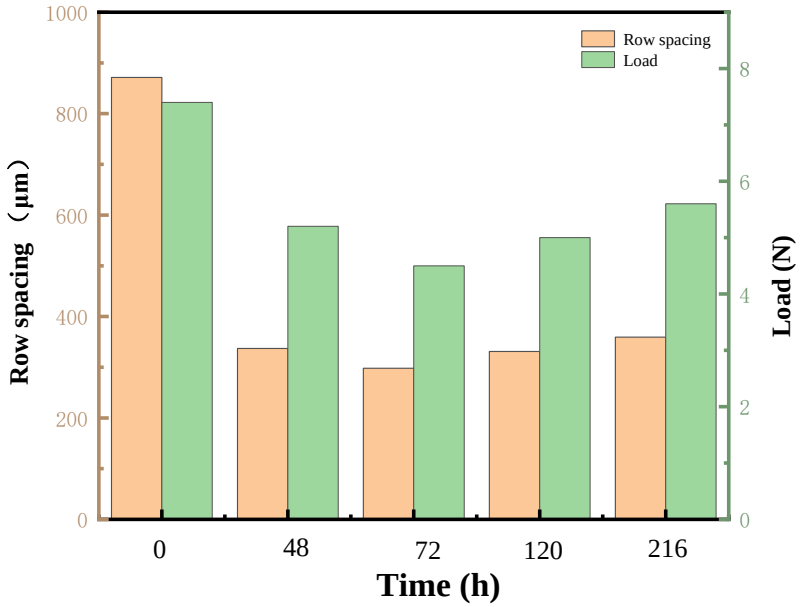
$$Al \rightarrow Al^{3+} + 3e^- \quad (5)$$

$$Al^{3+} + 3OH^- \rightarrow Al(OH)_3 \quad (6)$$

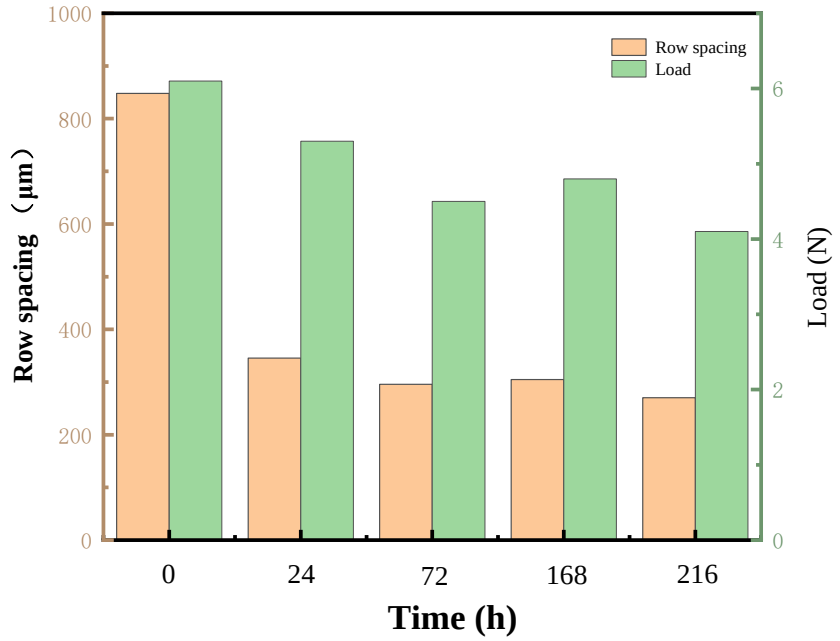
As the salt-spray test continued $Zn_5(OH)_8Cl_2$ was finally formed on the cold-spray *Al-Zn* coating; the reaction equation is the same as (4) [32]. After the salt-spray test, $Zn_5(OH)_8Cl_2$ was the main corrosion product on the cold-spray Al-Zn coating, but not on hot-dip zinc and hot-spray zinc coatings. This phenomenon was caused by the fact that the increase in Al can promote the formation of $Zn_5(OH)_8Cl_2$ [33]. Due to the above electrode reactions, a large number of electron-losing metal positive ions gathered in the pores of the coating. Under the action of the electric field, some Cl^- with small radius penetrated through the corrosion products into the coating. The combined action of H^+ and Cl^- intensified the local corrosion of the coating, thus reducing the corrosion resistance of the coating [34].

3.4. Adhesion Analysis

In terms of the protection performance of the coating, the greater the adhesion between the coating and the substrate, the better the protection performance of the coating on the substrate, which improves the corrosion resistance of the coating and prolongs the service life of the coating. In this paper, the adhesion of hot-dip zinc, hot-spray zinc and cold-spray aluminum zinc coatings after the salt-spray test was determined by the method of scratch test. The critical load and row spacing of the three metal coatings after the salt-spray test are shown in Figure 7.

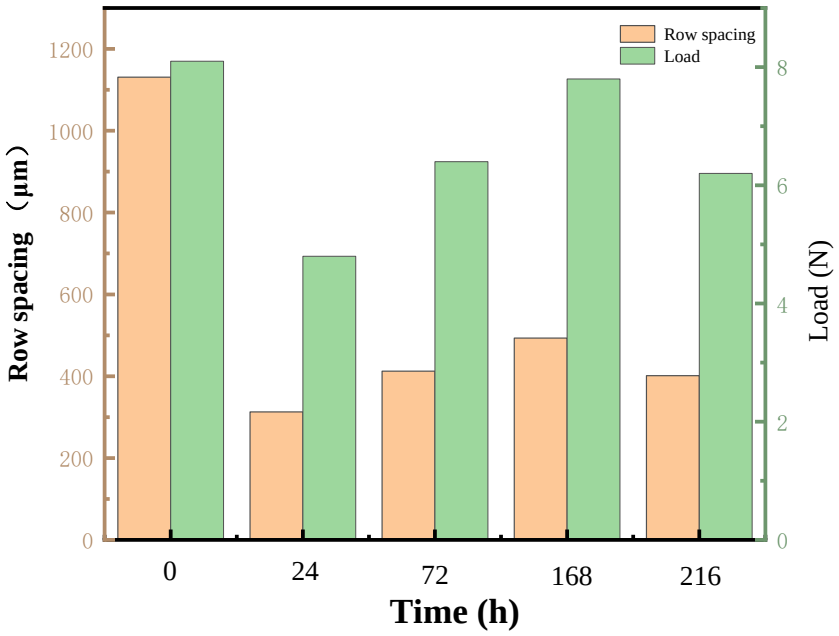


(**a**)



(**b**)

Figure 7. *Cont.*



(**c**)

Figure 7. Adhesion and row spacing of the three metal coatings after salt-spray test. (**a**) Hot-dip zinc, (**b**) hot-spray zinc, and (**c**) cold-spray aluminum zinc coatings.

The critical loads of hot-dip zinc, hot-spray zinc and cold-spray aluminum-zinc coatings fluctuated up and down in the salt-spray test, and the basic trend was first decreasing, then increasing and then decreasing. The critical load decreased first because the passivation film on the surface of the coating was corroded and the coating dissolved. Then, the corrosion products accumulated on the surface of the coating to form a passivation film, and the adhesion of the coating increased. Finally, the adhesion of the coating decreased because the corrosion products gradually flaked off. It can be seen that the critical loads of the cold-spray *Al-Zn* coating was higher than those of the other two coatings. This is because the process of preparation of cold spray aluminum zinc coating has lower temperature, therefore, the coating metal particles have a lower oxidation degree. After the substrate is covered and deposited by the sprayed metal particles, the subsequently sprayed particles have a high flight-speed impact on the deposited coating. The hard-phase alumina in the cold-spray aluminum zinc has a tamping effect on the impact of the coating. The impact and collision between metal particles make the local temperature rise instantaneously, and then metallurgical bonding occurs, which improves the binding property of the coating [35]. Moreover, the compactness of cold-spray aluminum-zinc coating is higher than that of hot-dip zinc and hot-spray zinc coatings, so the adhesion of cold spray aluminum-zinc coating is higher than that of hot-dip zinc and hot-spray zinc coatings, which is more conducive to strengthening the protection performance of the coating on the substrate, improving the corrosion resistance of the coating and extending the service life of the coating.

3.5. Weight Loss Measurement

The weight loss of the three metal coatings in the salt-spray test is shown in Figure 8. The weight of the three metal coating samples in the salt-spray test is downward. After salt-spray testing for 24 h, the weight loss of the three metal coatings was large, and the corrosion rate was fast. The weight loss of hot-dip zinc coating was the largest, indicating that the corrosion rate of the hot-dip zinc coating was the highest within 24 h of the salt-spray test. As the salt-spray test continued, the weight loss of the hot-dip zinc coating decreased first, and then increased after 72 h of the salt-spray test. The reason for the reduction in weight loss is that the corrosion products attached to the coating effectively

prevented the corrosion medium and reduced the corrosion rate of the coating. The weight loss increased because the corrosion products on the coating were continuously dissolved, and the physical shielding effect decreased. As the salt-spray test time increased, the weight loss of the hot-spray zinc coating and the cold-spray aluminum zinc coating increased slowly, and the corrosion rate of the coatings also decreased gradually and tended to be stable, indicating that the continuous formation and dissolution of the passive film occurred after the corrosion of the coating surface.

The weight loss of the cold-spray aluminum zinc coating was the most stable and minimal in the salt-spray test, while the weight loss of the hot-dip zinc coating was the largest and fluctuated the most in the salt-spray test, indicating that the corrosion rate of the cold-spray aluminum zinc coating was minimal, and the corrosion rate of the hot-dip zinc coating was maximal. To sum up, the corrosion resistance of the cold-spray aluminum zinc coating was better than that of the hot-dip zinc and hot-spray zinc coatings, and the corrosion resistance of the hot-dip zinc coating is the weakest.

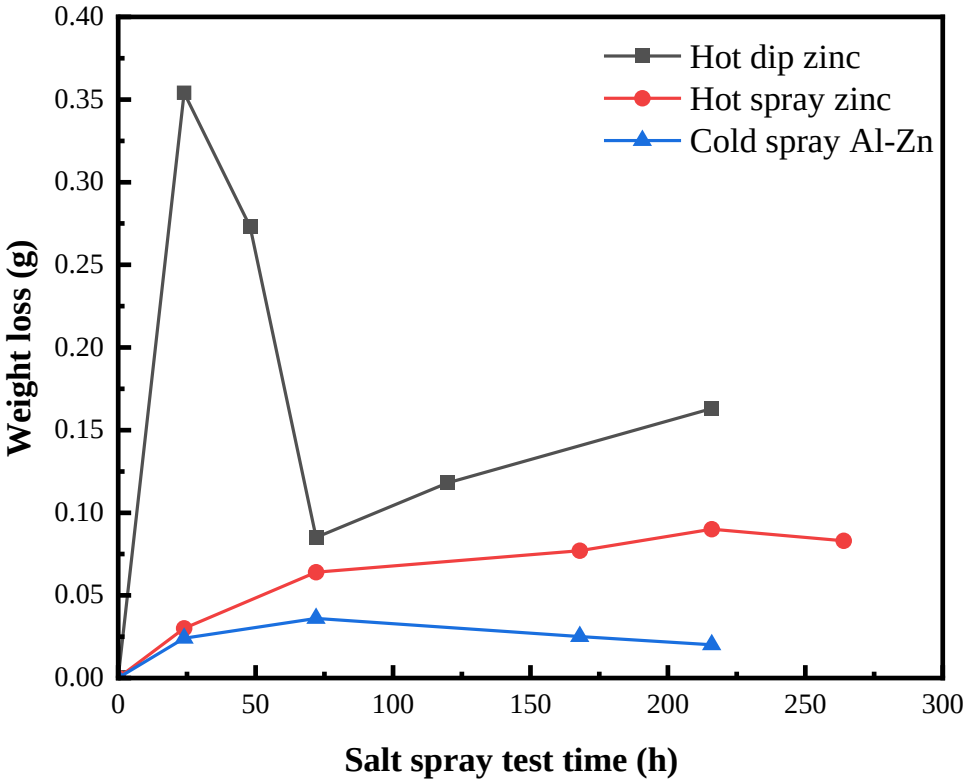


Figure 8. Weight loss of three metal coatings in salt-spray test.

3.6. Electrochemical Performance Analysis

The polarization curves of the salt-spray test for three metal coatings are shown in Figure 9. For metal electrodes used for corrosion in electrochemistry, the anodic and cathodic reactions generally follow the Tafel rule, and the corrosion polarization equation is derived as follows:

$$i_a = i_{corr}\left[\exp\left(\frac{E - E_{corr}}{\beta_a}\right) - \exp\left(\frac{E_{corr} - E}{\beta_c}\right)\right] \quad (7)$$

$$i_c = i_{corr}\left[\exp\left(\frac{E_{corr} - E}{\beta_c}\right) - \exp\left(\frac{E - E_{corr}}{\beta_a}\right)\right] \quad (8)$$

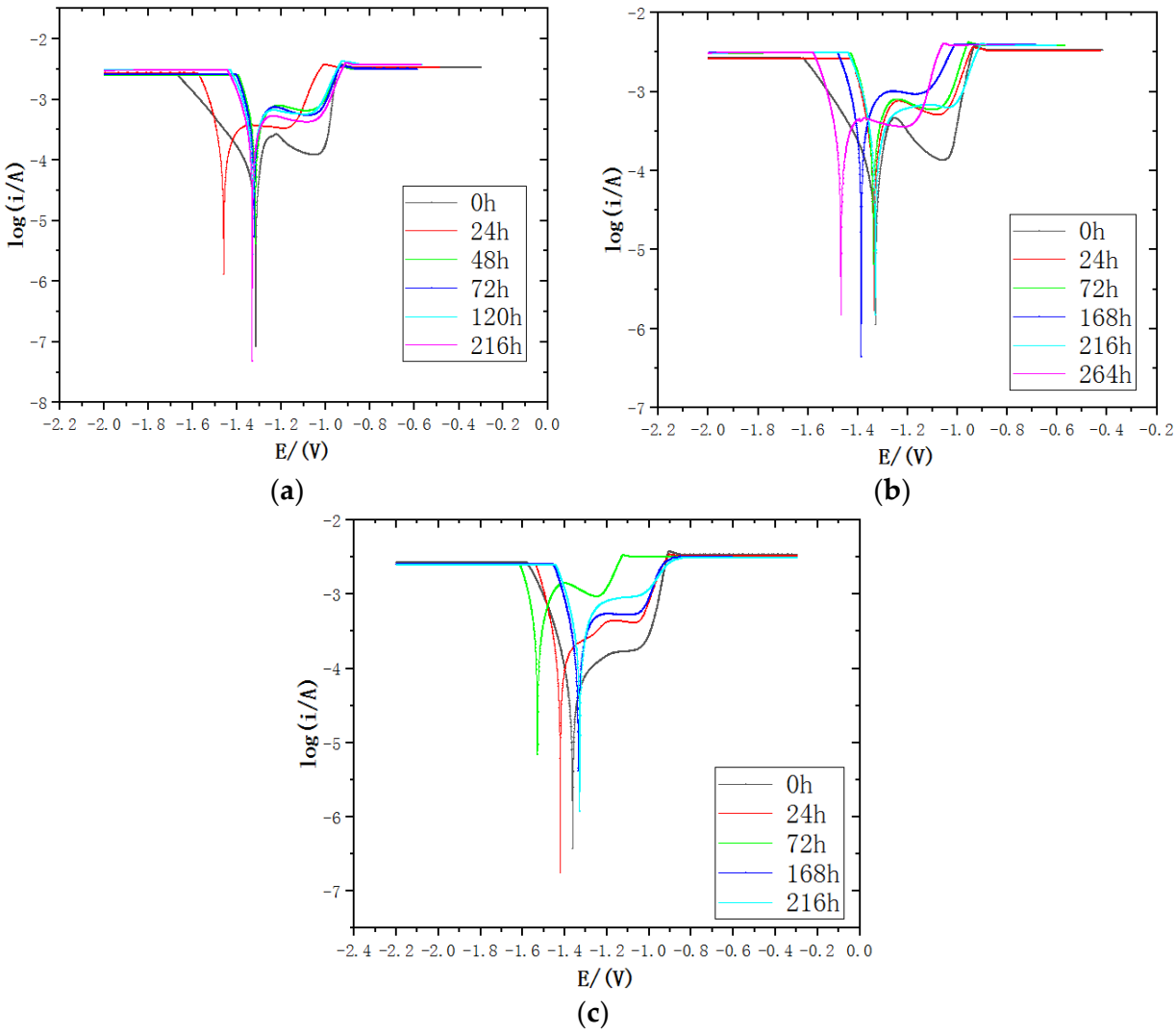


Figure 9. Polarization curves of salt-spray test for three metal coatings. (**a**) Hot-dipping zinc, (**b**) hot-spraying zinc and (**c**) cold-spraying aluminum zinc.

And $i_a = i_c = i_{corr}$. According to Stern–Geary formula [36], we know:

$$B = \frac{\beta_a \times \beta_c}{2.303 \times (\beta_a + \beta_c)} \tag{9}$$

$$i_{corr} = \frac{B}{R_p} \tag{10}$$

R_p represents the polarization resistance, B represents the Stern–Geary constant and β_a and β_c are the anode and cathode Tafel constant, respectively. Self-corrosion current density (i_{corr}) can reflect the size of the corrosion resistance of metal electrode materials: the smaller the value, the better the corrosion resistance.

The cathodic polarization curves and anode polarization curves of the three coatings of hot-dip zinc, hot-spray zinc and cold-spray aluminum zinc were fitted. The intersection of the fitting lines was the corrosion potential and corrosion current density of the coating. The results are shown in Tables 1–3. It can be seen from the table that the corrosion potential of the hot-dip zinc coating and hot-spray zinc coating decreased first, then increased, and then finally decreased during the 216 h salt-spray test, while the corrosion potential of the cold-spray aluminum zinc coating decreased first and then increased.

Table 1. Self-corrosion potential and corrosion current density of hot-dip zinc coating after each time period of salt-spray test.

Salt Spray Time/h	E/V	(i/A)/(A/cm^2)
0	−1.34	1.58×10^{-4}
24	−1.46	2.32×10^{-4}
48	−1.32	3.69×10^{-4}
72	−1.32	3.88×10^{-4}
120	−1.33	3.67×10^{-4}
216	−1.33	2.93×10^{-4}

Table 2. Self-corrosion potential and corrosion current density of hot-spray zinc coating after each time period of salt-spray test.

Salt Spray Time/h	E/V	(i/A)/(A/cm^2)
0	−1.33	9.33×10^{-5}
24	−1.34	1.80×10^{-4}
72	−1.34	3.77×10^{-4}
168	−1.39	3.84×10^{-4}
216	−1.33	4.87×10^{-4}
264	−1.47	2.47×10^{-4}

Table 3. Self-corrosion potential and corrosion current density of cold-spray Al-Zn coating after each time period of salt-spray test.

Salt Spray Time/h	E/V	(i/A)/(A/cm^2)
0	−1.36	5.75×10^{-5}
24	−1.44	1.22×10^{-4}
72	−1.53	4.56×10^{-4}
168	−1.34	1.36×10^{-4}
216	−1.33	2.43×10^{-4}

The corrosion current density of the hot-dip zinc coating increased during the salt-spray test for 72 h, and decreased during the salt-spray test between 72 h and 216 h. The corrosion current density of the hot-spray zinc coating increased during the 216 h salt-spray test, and decreased between 216 h and 264 h in the salt-spray test. The corrosion current density of the cold-sprayed aluminum zinc coating increased during the salt-spray test for 72 h, while the corrosion current density decreased during the salt-spray test between 72 h and 168 h, and then increased. This phenomenon was caused by the corrosion spalling of the protective film of the oxide layer on the coating at the initial stage of the salt-spray test. Later, with the progress of the salt-spray test, the corrosion products on the coating accumulated and dissolved spalling. Moreover, at the same salt-spray timepoint, the corrosion current density of the cold-spray aluminum zinc coating was almost entirely greater than that of the hot-dip zinc coating and hot-spray zinc coating, so the corrosion resistance of the cold-spray aluminum zinc coating was better than the other two coatings.

4. Conclusions

(1) A layer of islands and granular corrosion products were formed on the surface of the hot-dip zinc and hot-spray zinc coatings after salt-spray test corrosion, with loose structure and uneven distribution. The cracks in the grain boundaries of the coating led to obvious cracking and spalling of the corrosion products, and the physical shielding effect on the corrosive medium was poor. After the salt-spray test, the surface of the cold-spray aluminum zinc coating was almost covered by corrosion products, with dense structure and uniform distribution. The grain size of the Al particles was different from that of *Zn*

particles. After corrosion, the particle bonding property became weak, leading to obvious cracks on the coating surface. However, the flocculent corrosion products covered the cracks and had a good physical shielding effect on the corrosive medium. Therefore, the corrosion resistance of cold-spray aluminum-zinc coating was better than that of the hot-dip zinc and hot-spray zinc coatings.

(2) The critical loads of hot-dip zinc, hot-spray zinc and cold-spray aluminum-zinc coatings fluctuated up and down in the salt-spray test, and the basic trend was first decreasing, then increasing and then decreasing. The critical load of the cold-spray aluminum-zinc coating over 216 h of salt-spray test was higher than that of the other two coatings. Moreover, the compactness of cold-spray aluminum-zinc coating was greater than that of the hot-dip zinc and hot-spray zinc coatings, so the adhesion of the cold spray aluminum-zinc coating was greater than that of the hot-dip zinc and hot-spray zinc coatings, which was more conducive to strengthening the protection performance of the coating on the substrate, improving the corrosion resistance and extending the service life of the coating.

(3) The weight of the three metal coating samples in the salt-spray test was downward. The weight loss of the cold-spray aluminum zinc coating was the most stable and minimal in the salt-spray test, while the weight loss of the hot-dip zinc coating was the largest and fluctuated the most in the salt-spray test, indicating that the corrosion rate of the cold-spray aluminum zinc coating was minimal, and the corrosion rate of the hot-dip zinc coating was maximal. Therefore, the corrosion resistance of the cold-spray aluminum-zinc coating was better than that of the hot-dip zinc and hot-spray zinc coatings, and the corrosion resistance of the hot-dip zinc coating was the poorest.

(4) In the salt-spray test of the three metal coatings, the corrosion current density increased first and then decreased. At the same salt-spray timepoint, the corrosion current density of the cold-spray aluminum zinc coating was smaller than that of the hot-dip zinc coating and hot-spray zinc coating. Therefore, the corrosion tendency of the cold-spray aluminum zinc coating was lower than that of the hot-dip zinc coating and hot-spray zinc coating, which can provide longer service time for the substrate and better corrosion resistance.

Author Contributions: Conceptualization, B.Y.; methodology, H.W.; software, B.L.; validation, Q.H., T.S. and R.Y.; formal analysis, J.C. and J.L.; investigation, B.W.; resources, Y.L. and G.Z.; data curation, J.C. and J.L.; writing—original draft preparation, J.L.; writing—review and editing, J.C., J.L. and B.Y.; visualization, Q.W.; supervision, Z.L.; project administration, B.Y.; funding acquisition, B.Y. All authors have read and agreed to the published version of the manuscript.

Funding: This research was funded by the Science and Technology Project of China Southern Power Grid (GZKJXM20191302).

Institutional Review Board Statement: Not applicable.

Informed Consent Statement: Not applicable.

Data Availability Statement: Not applicable.

Conflicts of Interest: The authors declare no conflict of interest.

References

1. Chen, X.F.; Zhang, Z.Y.; Zhang, H.P.; Yan, H.B.; Liu, F.C.; Tu, S. Influence of Air Pollution Factors on Corrosion of Metal Equipment in Transmission and Transformation Power Stations. *Atmosphere* **2022**, *13*, 1041. [CrossRef]
2. Rodger, J.; Bartlett, S.; Atrens, A. Corrosion of the galvanizing of galvanized-steel electricity transmission towers. *Mater. Corros.-Werkst. Und Korros.* **2017**, *68*, 902–910. [CrossRef]
3. Yu, J.S.; Guo, J.K.; Zhao, P.; Lu, L.Q. Environmental corrosiveness evaluation and corrosion charactistics analysis of power transmission and transformation equipment. In Proceedings of the 2014 China International Conference on Electricity Distribution (CICED), Shenzhen, China, 23–26 September 2014.
4. Gu, Y.; Li, N.; Zhang, F.G.; Li, L. Corrosion and Protection of Submarine Metal Components in Seawater. In Proceedings of the 2009 8th International Conference on Reliability, Maintainability and Safety, Chengdu, China, 20–24 July 2009; pp. 1226–1229.
5. Xu, N.X.; Zhao, L.Y.; Ding, C.H.; Zhang, C.D.; Li, R.S.; Zhong, Q.D. Laboratory observation of dew formation at an early stage of atmospheric corrosion of metals. *Corros. Sci.* **2002**, *44*, 163–170. [CrossRef]

6. Li, C.L.; Ma, Y.T.; Li, Y.; Wang, F.H. EIS monitoring study of atmospheric corrosion under variable relative humidity. *Corros. Sci.* **2010**, *52*, 3677–3686. [CrossRef]
7. Valverde, B.; Vera, R.; Henriquez, N.; Olave, E. Evaluation of atmospheric galvanic aluminum corrosion in electrical transmission towers at different sites in the Valparaiso region, Chile. Wire-on-Bolt Test (CLIMAT). *Mater. Corros.-Werkst. Und Korros.* **2021**, *72*, 1607–1619. [CrossRef]
8. Wang, B.; Zhang, L.W.; Jiang, H.; Li, X.B.; Mu, X.L. Atmospheric corrosion comparison of antirust aluminum exposed to industrial and coastal atmospheres. *Mater. Corros.-Werkst. Und Korros.* **2018**, *69*, 1516–1525. [CrossRef]
9. Balakrishnan, K. Trends in corrosion protection of materials. *Bull. Mater. Sci.* **1994**, *17*, 1331–1339. [CrossRef]
10. Chakir, A.; Koch, H.; IEEE. Corrosion protection for gas-insulated transmission lines. In Proceedings of the IEEE Power Engineering Society Summer Meeting, Chicago, IL, USA, 21–25 July 2002; pp. 220–224.
11. Chu, C.T.; Alaan, D.R.; Taylor, D.P. Accelerated atmospheric corrosion testing of electroplated gold mirror coatings. In Proceedings of the Conference on Current Developments in Lens Design and Optical Engineering XI; and Advances in Thin Film Coatings VI, San Diego, CA, USA, 1–3 August 2010.
12. Li, S.; Yan, J.Y.; Wang, X.G. On comparison between reinforcement electricity accelerated corrosion and natural corrosion of concrete. *Appl. Mech. Mater.* **2013**, *357–360*, 676–679. [CrossRef]
13. Bao, Z.B.; Wang, Q.M.; Jiang, S.M.; Gong, J.; Sun, C. Influence of salt spray corrosion on subsequent isothermal oxidation behaviours of AIP NiCoCrAlYSiB coatings. *Corros. Sci.* **2008**, *50*, 2372–2380. [CrossRef]
14. Wang, X.; Xu, S.J.; Wang, J.Y.; Ren, K.X.; Liu, P. Environmental Corrosion Behavior and Accelerated Corrosion Verification of Metal Part. In Proceedings of the 2nd IYSF Academic Symposium on Artificial Intelligence and Computer Engineering, Xi'an, China, 8–10 October 2021.
15. Onye, J.; Frankel, G.S. Effects of NaCl, SO_2, NH_3, O_3, and ultraviolet light on atmospheric corrosion of Zn. *Mater. Corros.-Werkst. Und Korros.* **2020**, *71*, 9–20. [CrossRef]
16. Qu, Q.; Yan, C.W.; Wan, Y.; Cao, C.N. Effects of NaCl and SO_2 on the initial atmospheric corrosion of zinc. *Corros. Sci.* **2002**, *44*, 2789–2803. [CrossRef]
17. Svensson, J.E.; Johansson, L.G. AA laboratory study of the initial stages of the atmospheric corrosion of zinc in the presence of NaCl; Influence of SO_2 and NO_2. *Corros. Sci.* **1993**, *34*, 721–740. [CrossRef]
18. Lindstrom, R.; Svensson, J.E.; Johansson, L.G. The atmospheric corrosion of zinc in the presence of NaCl the influence of carbon dioxide and temperature. *J. Electrochem. Soc.* **2000**, *147*, 1751–1757. [CrossRef]
19. Witharamage, C.S.; Alrizqi, M.A.; Chirstudasjustus, J.; Darwish, A.A.; Ansell, T.; Nieto, A.; Gupta, R.K. Corrosion-resistant metallic coatings for aluminum alloys by cold spray. *Corros. Sci.* **2022**, *209*, 110720. [CrossRef]
20. Li, Y.T.; Yang, L.H.; Li, X.; Liu, J.G.; Hou, B.R. Corrosion Behavior of Sprayed Zinc-Aluminum (ZZA) Coatings in Simulated Marine Environment. *Int. J. Electrochem. Sci.* **2013**, *8*, 9886–9893.
21. Chavan, N.M.; Kiran, B.; Jyothirmayi, A.; Phani, P.S.; Sundararajan, G. The Corrosion Behavior of Cold Sprayed Zinc Coatings on Mild Steel Substrate. *J. Therm. Spray Technol.* **2013**, *22*, 463–470. [CrossRef]
22. Xie, C.; Li, H.X.; Zhou, X.L.; Sun, C.C. Corrosion behavior of cold sprayed pure zinc coating on magnesium. *Surf. Coat. Technol.* **2019**, *374*, 797–806. [CrossRef]
23. Yoo, J.D.; Ogle, K.; Volovitch, P. The effect of synthetic zinc corrosion products on corrosion of electrogalvanized steel: I. Cathodic reactivity under zinc corrosion products. *Corros. Sci.* **2014**, *81*, 11–20. [CrossRef]
24. Rao, V.S. A review of the electrochemical corrosion behaviour of iron aluminides. *Electrochim. Acta* **2004**, *49*, 4533–4542. [CrossRef]
25. de Rincon, O.; Rincon, A.; Sanchez, M.; Romero, N.; Salas, O.; Delgado, R.; Lopez, B.; Uruchurtu, J.; Marroco, M.; Panosian, Z. Evaluating Zn, Al and Al-Zn coatings on carbon steel in a special atmosphere. *Constr. Build. Mater.* **2009**, *23*, 1465–1471. [CrossRef]
26. Zhu, F.; Persson, D.; Thierry, D. Formation of corrosion products on open and confined metal surfaces exposed to periodic wet/dry conditions—A comparison between zinc and electrogalvanized steel. *Corrosion* **2001**, *57*, 582–590. [CrossRef]
27. Petersen, R.B.; Wells, T.; Melchers, R.E. Development of long-term localised corrosion of cast iron pipes in backfill soils based on time of wetness. *Corros. Eng. Sci. Technol.* **2020**, *55*, 550–561. [CrossRef]
28. Zhu, F.; Persson, D.; Thierry, D.; Taxen, C. Formation of corrosion products on open and confined zinc surfaces exposed to periodic wet/dry conditions. *Corrosion* **2000**, *56*, 1256–1265. [CrossRef]
29. Del Angel, E.; Vera, R.; Corvo, F. Atmospheric Corrosion of Galvanised Steel in Different Environments in Chile and Mexico. *Int. J. Electrochem. Sci.* **2015**, *10*, 7985–8004.
30. Liu, Y.; Zhu, Z.X.; Chen, Y.X.; Xu, B.S.; Ma, S.N.; Li, Z.X. Electrochemical corrosion behavior of arc sprayed Zn-Al coatings. *Trans. Nonferrous Met. Soc. China* **2004**, *14*, 443–445.
31. Shaw, B.A.; Moran, P.J. Characterization of the corrosion behavior of zinc-aluminum thermal spray coatings. *Mater. Perform.* **1985**, *24*, 22–31.
32. El-Mahdy, G.A.; Nishikata, A.; Tsuru, T. AC impedance study on corrosion of 55%Al-Zn alloy-coated steel under thin electrolyte layers. *Corros. Sci.* **2000**, *42*, 1509–1521. [CrossRef]
33. Rosalbino, F.; Angelini, E.; Maccio, D.; Saccone, A.; Delfino, S. Application of EIS to assess the effect of rare earths small addition on the corrosion behaviour of Zn-5% Al (Galfan) alloy in neutral aerated sodium chloride solution. *Electrochim. Acta* **2009**, *54*, 1204–1209. [CrossRef]

34. Moreira, A.R.; Panossian, Z.; Camargo, P.L.; Moreira, M.F.; da Silva, I.C.; de Carvalho, J.E.R. Zn/55Al coating microstructure and corrosion mechanism. *Corros. Sci.* **2006**, *48*, 564–576. [CrossRef]
35. Wang, S.D.; Xue, L.J.; Jiang, J.R. Cold sprayed aluminum and aluminum alloy coatings. In Proceedings of the Tms 2009 138th Annual Meeting and Exhibition-Supplemental Proceedings, Vol 1: Materials Processing and Properties, San Francisco, CA, USA, 15–19 February 2009; pp. 413–420.
36. Sun, Y.P.; Yang, C.T.; Yang, C.G.; Xu, D.K.; Li, Q.; Yin, L.; Qiu, C.S.; Liu, D.; Yang, K. Stern-Geary Constant for X80 Pipeline Steel in the Presence of Different Corrosive Microorganisms. *Acta Metall. Sin. (Engl. Lett.)* **2019**, *32*, 1483–1489. [CrossRef]

Disclaimer/Publisher's Note: The statements, opinions and data contained in all publications are solely those of the individual author(s) and contributor(s) and not of MDPI and/or the editor(s). MDPI and/or the editor(s) disclaim responsibility for any injury to people or property resulting from any ideas, methods, instructions or products referred to in the content.